Journal of Vacuum Science Technology A

ACCEPTED MANUSCRIPT

This is the author's peer reviewed, accepted manuscript. However, the online version of record will be different from this version once it has been copyedited and typeset.

PLEASE CITE THIS ARTICLE AS DOI: 10.1116/6.0000877

Effect of Metal Contacts on (100) β-Ga_2O_3 Schottky Barriers

Luke A. M. Lyle[1], Kunyao Jiang[1], Elizabeth V. Favela[1], Kalyan Das[2], Andreas Popp[3], Zbigniew Galazka[3], Guenter Wagner[3], Lisa M. Porter[1]

[1] Department of Materials Science and Engineering, Carnegie Mellon University, Pittsburgh, Pennsylvania, United States

[2] Department of Materials Science and Engineering, North Carolina State University, Raleigh, North Carolina, United States

[3] Leibniz-Institut für Kristallzchtüng, Berlin, Germany

The Schottky barriers of Ti, Mo, Co, Ni, Pd, and Au on (100) β-Ga_2O_3 substrates were analyzed using a combination of current-voltage (J-V), capacitance-voltage (C-V) and current-voltage-temperature (J-V-T) measurements. Near-ideal, average ideality factors for Ti, Mo, Co, and Ni were 1.05 – 1.15; whereas higher ideality factors (~1.3) were observed for Pd and Au contacts. Barrier heights ranging from 0.60 eV to 1.20 eV were calculated from J-V measurements for the metals with low ideality factors. C-V measurements of all Schottky metals were conducted and yielded average barrier heights ranging from 0.78 eV to 1.98 eV. J-V-T measurements of Ti and Co diodes yielded barrier heights of 0.81 and 1.35 eV, respectively. The results reveal a strong positive correlation between the calculated Schottky barrier heights and the metal work functions: the index of interface behavior, S = 0.70, 0.97, and 0.81 for the J-V, C-V, and J-V-T data, respectively.

I. INTRODUCTION

Beta-gallium oxide (β-Ga_2O_3) is a semiconductor that has garnered interest over the past decade due to its ultrawide bandgap (~4.6-4.9 eV) [1], wide range of n-type doping [2-5] (Si, Ge, Sn), and its ability to be produced as large-area, melt-grown substrates that serve as a platform for device-quality epitaxial layers [6-8]. For these reasons Ga_2O_3 is being pursued for high power devices [9] and UV photodetectors [10]. Other wide bandgap semiconductors such as GaN and SiC suffer from higher costs to produce substrates from vapor phase growth methods. In addition, Ga_2O_3 has a higher theoretical breakdown field (~8 MV/cm) and Baliga figure of merit (~3400) than GaN and SiC [11].

Studies of Schottky contacts to β-Ga_2O_3 play a fundamental role in designing metal-semiconductor field-effect transistors [12] and Schottky diodes [13]. As such, it's important to develop contacts with high Schottky barrier heights and low leakage currents. Metals with a wide range of work functions have been explored as Schottky contacts to Ga_2O_3, including W [14], Cu [15], Ni [16], Au [17], Pt [18], TiN [19], Pd [20], Ir [21], Ag [20], and Mo [22]. Similarly, Schottky contacts to (100), (010), (001), and $(\bar{2}01)$ orientations of β-Ga_2O_3 substrates grown via edge defined film fed growth [23, 24], Czochralski [16, 25], and floating zone [26], and to β-Ga_2O_3 epitaxial layers grown via metalorganic chemical vapor deposition [27-30], halide vapor phase epitaxy[6, 28], and pulsed laser deposition [31] have been reported. Yao et al. investigated five different Schottky metals to $(\bar{2}01)$ β-Ga_2O_3 substrates and found that the metal work function was not a strong indicator of the Schottky barrier height [18]. In a subsequent study authors examined

Journal of Vacuum Science Technology A
ACCEPTED MANUSCRIPT
This is the author's peer reviewed, accepted manuscript. However, the online version of record will be different from this version once it has been copyedited and typeset.
PLEASE CITE THIS ARTICLE AS DOI: 10.1116/6.0000877

oxidized and pure (unoxidized) metal contacts to $(\bar{2}01)$ β-Ga_2O_3 and also concluded the work function was not a strong indicator of Schottky barrier height [20]. Whereas Farzana et al. established evidence that the Fermi level is not completely pinned for Ni, Pd, and Pt Schottky contacts to the (010) β-Ga_2O_3 surface [32], other data suggest the metal work function is not a strong indicator of Schottky barrier height on the (010) β-Ga_2O_3 surface [21]. There is limited published work on Schottky contacts on the (100) [16, 17, 33-35] and (001) [36, 37] orientations of β-Ga_2O_3. In this work we measured the electrical behavior, at both room temperature and as a function of elevated temperature, of Ti, Mo, Co, Ni, Pd, and Au Schottky contacts to (100) β-Ga_2O_3 and calculated the Schottky barrier heights and ideality factors from these measurements. Observed trends are discussed and compared with previously published results for other Ga_2O_3 surfaces.

II. EXPERIMENT

N-type, unintentionally-doped (100) β-Ga_2O_3 single crystal wafers were grown by the Czochralski method at the Leibniz-Institut für Kristallzüchtung (IKZ) in Berlin, Germany. The as-received samples were 1 cm^2 and had resistivity, mobility, and free carrier concentration of 0.2 Ωcm, 60 cm^2/Vs, and 5 x 10^{17} cm^{-3}, respectively, as determined from Hall effect measurements. The doping concentration calculated from C-V measurements of Schottky diodes was 2.5–4.5 x 10^{17} cm^{-3}.

All metals were deposited onto unheated substrates by electron-beam evaporation (base pressure of ~10^{-8} Torr). Ohmic contacts were formed using Ti/Au (20nm/100nm) annealed at 450°C, either for 1 min. in N_2 in a rapid thermal annealing (RTA) furnace (for backside ohmic contacts, referred to below as vertical structures) or for 5 min. at 400°C in Ar in a resistively heated quartz tube furnace (for frontside ohmic contacts, referred to as the lateral structures). Prior to deposition of all Schottky contacts, each substrate was soaked in 10% hydrochloric acid (HCl) for 5 min, rinsed in deionized (DI) water, and immersed for 5 min. in boiling H_2O_2 at 85 °C. All samples were blown dry in nitrogen after each DI water rinse. The Schottky metals were subsequently deposited through a Mo shadow mask to form circular Schottky contacts with diameters of 125, 250, and 500 µm. Ti, Co, and Pd Schottky contacts were fabricated as vertical device structures with backside ohmic contacts, whereas Mo, Ni, and Au were fabricated as lateral structures with frontside ohmic contacts. The thickness of all deposited Schottky contacts is 30 nm. The Ti Schottky contacts were coated with 50 nm of Au to serve as a passivation layer.

Hall measurements were acquired using a MMR Technologies Hall Measurement System at room temperature. For these measurements Ti/Au (20 nm/50 nm) contacts were deposited in a van der Pauw pattern onto a (100) β-Ga_2O_3 substrate and annealed at 400 °C for 5 minutes in Ar. J-V and J-V-T measurements were obtained using an Agilent 4155C Semiconductor Parameter Analyzer and a Signatone S-1160A-4N probe station. C-V measurements were performed at 1 MHz using an HP 4284 LCR meter and a Signatone S-1160A-4N probe station.

III. RESULTS AND DISCUSSION

For Schottky contacts that follow the thermionic emission model, the current density (J) vs. voltage (V) behavior is described in equation 1:

$$J(V) = J_s[e^{\frac{q(V-IR_s)}{nkT}} - 1] \quad (1)$$

Journal of Vacuum Science Technology A
ACCEPTED MANUSCRIPT

This is the author's peer reviewed, accepted manuscript. However, the online version of record will be different from this version once it has been copyedited and typeset.
PLEASE CITE THIS ARTICLE AS DOI: 10.1116/6.0000877

where q is the electronic charge, I is the current, R_S is the series resistance, n is the ideality factor, and k is the Boltzmann constant. J_s is the saturation current density defined as

$$J_s = A^{**}T^2 e^{-\frac{q\phi_B^{JV}}{kT}} \quad 2$$

where A^{**} is the Richardson's constant for the semiconductor and ϕ_B^{JV} is the J-V determined Schottky barrier height. The Richardson constant for β-Ga_2O_3 has been calculated to be 33.65 A/cm^2K^2 [38].

Fig. 1(a) shows representative log-J vs. V characteristics for each Schottky metal under forward bias conditions. Most metals display linearity over several decades of current before reaching series resistance limitations. An exception is Au, which displays multiple linear regions, suggestive of an inhomogeneous Schottky barrier, as established by other authors on other β-Ga_2O_3 surfaces [18, 39].

Ideality factors and Schottky barrier heights were calculated from J-V characteristics using the Cheung and Cheung method [40]. This method uses a plot of

$$\frac{dV}{d\ln J} = JAR_S - \frac{nkT}{q} \quad 3$$

where A = diode area, to extract n from the y-intercept of a $\frac{dV}{d\ln J}$ vs. J plot; and a function

$$H(J) \equiv V - \frac{nkT}{q}\ln\left(\frac{J}{A^{**}T^2}\right) = JAR_S - n\phi_B^{JV} \quad 4$$

from which ϕ_B^{JV} is determined from the y-intercept of a $H(J)$ vs. J plot. Table 1 lists the ϕ_B^{JV} values for Ti, Mo, Co, and Ni Schottky metal contacts, along with the ideality factors and the leakage current density values at -5 V for all Schottky contacts. Because of the higher ideality factors for Pd and Au contacts, the calculated Φ_B^{JV} values (1.42 ± 0.07 and 1.37 ± 0.09 eV, respectively) for these contacts do not follow thermionic emission and are not included in the analysis. The higher ideality factors for the Au and Pd contacts are associated with spatial inhomogeneity of the Schottky barriers for Au/Ga_2O_3 and Pd/Ga_2O_3 interfaces. Spatially inhomogeneous Schottky barriers are believed to result from Au-Ga and Pd-Ga alloy formation at the metal semiconductor interface. Pd-Ga and Au-Ga elemental formations have been reported on other Ga- based semiconductors including GaAs [41, 42] and GaN [43, 44]. The larger ideality factors observed for the Pd and Au contacts would be compatible with this phenomenon. Others have also reported evidence for an inhomogeneous Schottky barrier in Au Schottky contacts to (010) β-Ga_2O_3 [32]. Furthermore, our analysis of J-V-T measurements of Pd contacts, described below and in the Supplementary Information, indicates the presence of significant barrier inhomogeneity, as quantified by the standard deviation of the gaussian distribution, σ_0. The σ_0 value of the barrier shows a higher value for Pd than both Co and Ti, implying more variance in the measurements of the Schottky barrier height for Pd.

Schottky barrier heights were also calculated from C-V measurements. As derived from the depletion approximation [45]:

Journal of Vacuum Science Technology A
ACCEPTED MANUSCRIPT
This is the author's peer reviewed, accepted manuscript. However, the online version of record will be different from this version once it has been copyedited and typeset.
PLEASE CITE THIS ARTICLE AS DOI: 10.1116/6.0000877

$$\frac{A^2}{C(V)^2} = \frac{2\left(q\phi_B^{CV} - kT\ln\left(\frac{N_C}{N_d}\right) - qV - kT\right)}{q^2\varepsilon_s N_d} \qquad 5$$

where ϕ_B^{CV} , ε_s, and N_d, are the C-V determined Schottky barrier height, semiconductor permittivity, and doping concentration, respectively. N_c, the conduction band density of states, is expressed:

$$N_c = 2\left(\frac{2\pi m^* kT}{h^2}\right)^{\frac{3}{2}} \qquad 6$$

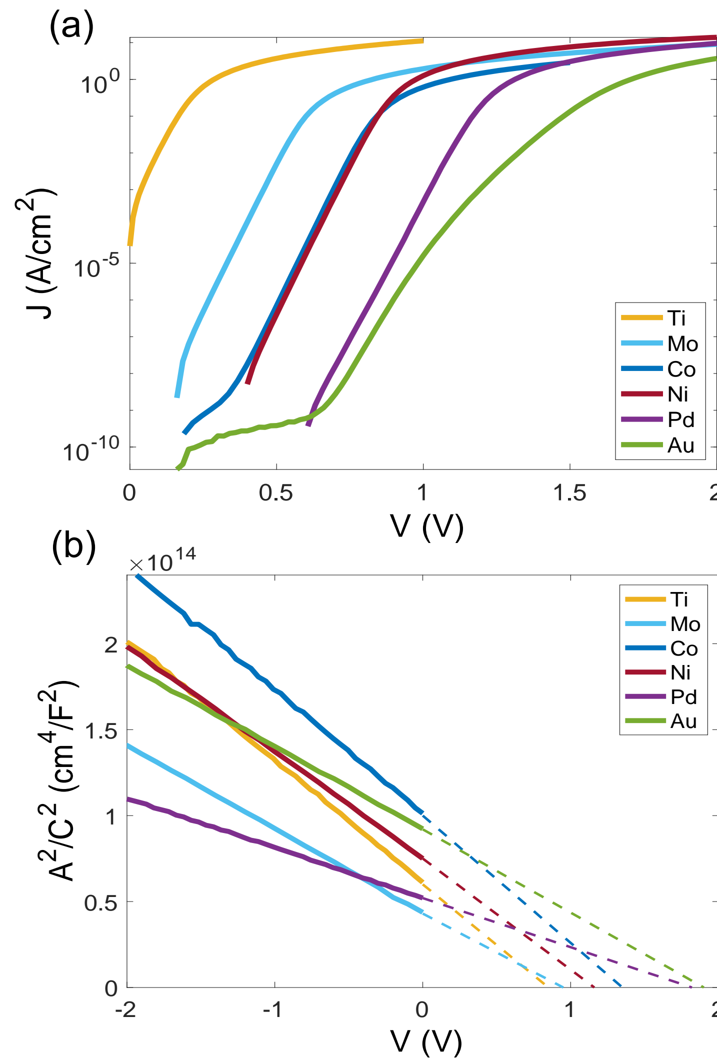

FIG. 1. (a) J-V and (b) C-V characteristics for Ti, Mo, Co, Ni, Pd, and Au Schottky contacts on (100) β-Ga_2O_3. The C-V data are plotted as diode area-squared divided by capacitance-squared vs. voltage to allow calculation of Schottky barrier heights for each metal. The diameter of each diode is 500 μm.

Journal of Vacuum Science Technology A
ACCEPTED MANUSCRIPT
This is the author's peer reviewed, accepted manuscript. However, the online version of record will be different from this version once it has been copyedited and typeset.
PLEASE CITE THIS ARTICLE AS DOI: 10.1116/6.0000877

Table 1. Electrical properties extracted from J-V, C-V, and J-V-T measurements. Where applicable, the standard deviations are indicated with +/- values.

Metal	Leakage Current @ -5V (A/cm^2)	n	ϕ_B^{JV} (eV)	ϕ_B^{Hom} (eV)	ϕ_B^{CV} (eV)	ϕ_B^{JVT} (eV)
Ti	7.64×10^{-2}	1.15 ± 0.05	0.60 ± 0.03	0.68	0.78 ± 0.08	0.81 ± 0.11
Mo	1.05×10^{-5}	1.05 ± 0.02	1.00 ± 0.02	0.99	0.95 ± 0.05	–
Co	6.67×10^{-9}	1.06 ± 0.01	1.20 ± 0.02	1.32	1.33 ± 0.10	1.35 ± 0.03
Ni	3.32×10^{-8}	1.05 ± 0.02	1.20 ± 0.03	1.25	1.25 ± 0.05	–
Pd	1.59×10^{-9}	1.26 ± 0.07	–*	1.62	1.86 ± 0.13	–*
Au	4.77×10^{-9}	1.32 ± 0.07	–*	1.41	1.98 ± 0.04	–

***:** The ideality factors obtained from I-V measurements were too large to attribute ϕ_B^{JV} to pure thermionic emission transport.

where $m^* = 0.28m_0$ is the electron effective mass in β-Ga_2O_3 and m_0 is the free electron mass. For β-Ga_2O_3 at room temperature the conduction band density of states is calculated to be $N_c = 2.67 \times 10^{18}\ cm^{-3}$. Therefore, by plotting A^2/C^2 vs. V (as shown in Fig. 1(b)), N_d can be calculated from the slope and the barrier height can be calculated from the x-intercept.

The C-V determined Schottky barrier heights are listed in Table 1, column 6. Note that differences in C-V and J-V determined barrier heights are commonly reported. For example, barrier heights from C-V measurements are typically higher than those calculated from J-V measurements. Tung [46] attribute this effect to slight nonidealities (or spatially inhomogeneous Schottky barriers) in the diodes. For Mo, Co, and Ni, the agreement between the C-V and J-V determined barrier heights are within 3–9%, whereas the agreement between these values for Ti is ~ 20–30%.

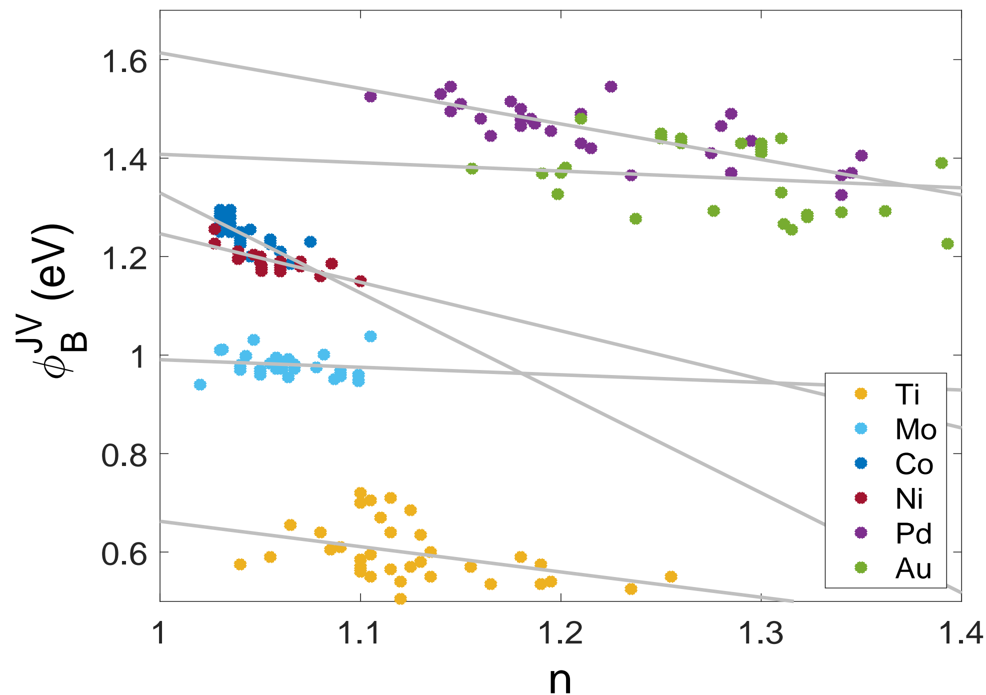

FIG. 2. J-V determined barrier heights for Ti, Mo, Co, Ni, Pd, and Au on (100) β-Ga_2O_3 plotted vs. ideality factor.

Journal of Vacuum Science Technology A
ACCEPTED MANUSCRIPT
This is the author's peer reviewed, accepted manuscript. However, the online version of record will be different from this version once it has been copyedited and typeset.
PLEASE CITE THIS ARTICLE AS DOI: 10.1116/6.0000877

A homogeneous Schottky barrier height, ϕ_B^{Hom}, can be defined by plotting ϕ_B^{JV} vs. n and extrapolating to n = 1, as shown in Fig. 2. This method [47] works well for diodes with low ideality factors. For example, the ϕ_B^{Hom} values (Table 1, column 5) for Ti, Mo, Co, and Ni are in relatively close agreement with the ϕ_B^{JV} and ϕ_B^{CV} values. For Pd, there is also reasonably close agreement between ϕ_B^{Hom} and Φ_B^{CV}, but for Au these values differ by ~0.5 eV.

We accounted for a spatial distribution of Schottky barriers in our analysis of J-V-T measurements of the vertical (Ti, Co, and Pd) device structures. As such, J-V-T measurements provided a potential third method to determine Schottky barrier heights for these diodes. However, as evidenced by the high ideality factors of the Pd diodes (~1.3), the current transport is not dominated by thermionic emission. Although minimum ideality factors of 1.10-1.15 are obtained in the 150-200 °C range was observed, corresponding to a calculated barrier height of ~1.7 eV at that temperature, the generally high ideality factors precluded a determination of a reliable Φ_B^{JVT} for the Pd contacts.

The J-V-T data for the vertical devices was fit using a model developed by Werner and Güttler [48], which assumes the measured Schottky barriers yield a normalized Gaussian spatial distribution, P(ϕ_B), with average barrier height, $\overline{\phi_B}$, and standard deviation, σ:

$$P(\phi_B) = \frac{1}{\sigma\sqrt{2\pi}} e^{-\frac{(\overline{\phi_B}-\phi_B)^2}{2\sigma^2}} \quad 7$$

By applying this model as detailed in the Supplementary Materials section at [URL will be inserted by AIP Publishing], we obtain the following J-V-T relationship:

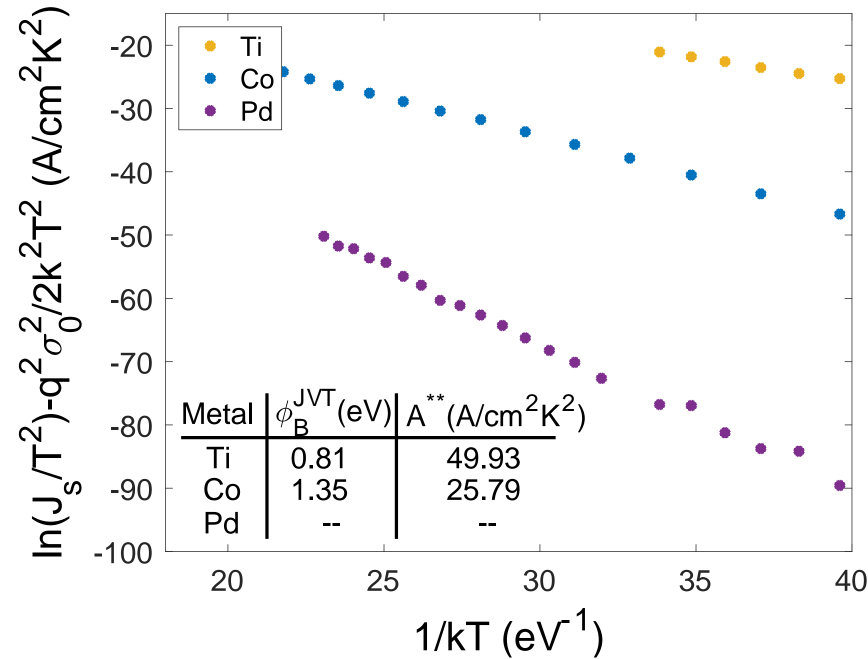

FIG. 3 (a) J-V-T characteristics for Schottky diodes with Ti and Co on (100) β-Ga_2O_3 plotted in accordance with the inhomogeneous Schottky barrier model described in Equation 8.

Journal of Vacuum Science Technology A
ACCEPTED MANUSCRIPT
This is the author's peer reviewed, accepted manuscript. However, the online version of record will be different from this version once it has been copyedited and typeset.
PLEASE CITE THIS ARTICLE AS DOI: 10.1116/6.0000877

$$\ln\left(\frac{J_s}{T^2}\right) - \frac{q^2\sigma_0^2}{2k^2T^2} = \ln A^{**} - \frac{q\phi_B^{JVT}}{kT} \quad (8)$$

where σ_0 is the standard deviation at zero bias and serves as a metric that determines the degree of spatial inhomogeneity of the Schottky barrier and also represents how strongly the Schottky barrier changes with temperature. σ_0 was determined to be 92, 72, and 197 meV for the Ti, Co, and Pd contacts, respectively. Fig. 3 plots the left-hand side of equation 8 vs. 1/kT, which provides a graphical method to calculate both the Richardson's constant of β-Ga_2O_3 (see Fig. 3 inset table) and the ϕ_B^{JVT} values (listed in the last column of Table 1). The Richardson's constant values calculated from this experimental data are in reasonable agreement with the theoretical value of β-Ga_2O_3 of 33.65 A/cm^{2}K^2 [38]. The near linear behavior of the curves in Figure 3 indicates that this model fits our data well.

The Schottky barrier heights calculated from the J-V, C-V, and J-V-T measurements discussed above are plotted vs. the metal work functions in Fig. 4. The black dashed line in the lower part of the plot represents the Schottky-Mott theory for an ideal metal-semiconductor contact:

$$\phi_B = \phi_M - \chi_s \quad (9)$$

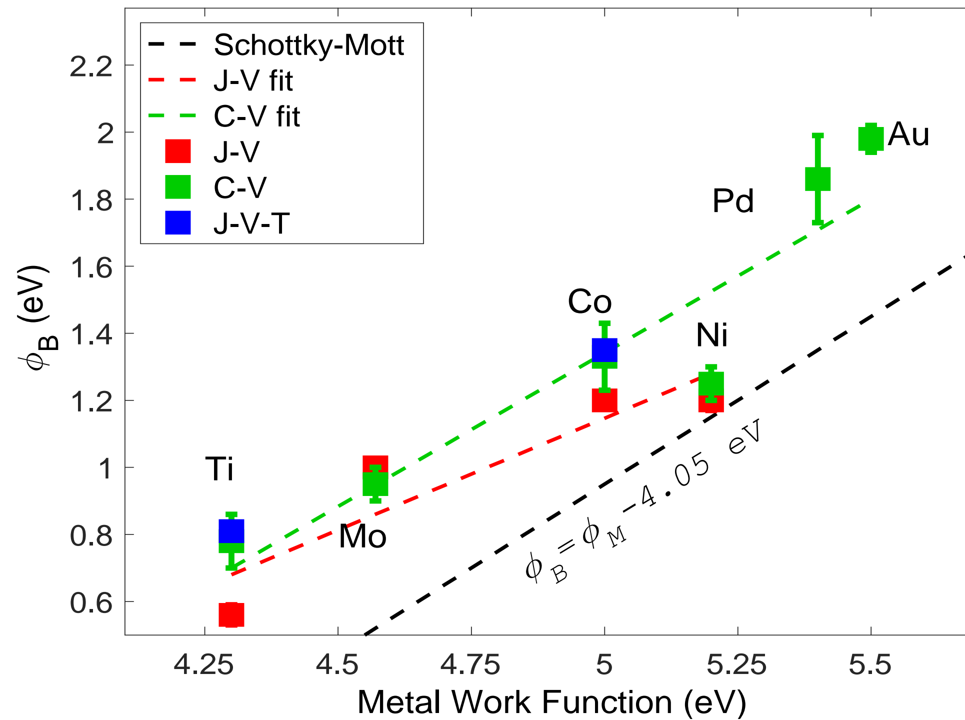

FIG. 4. Schottky barrier heights of Ti, Mo, Co, Ni, Pd and Au on (100) β-Ga_2O_3 plotted vs. metal work function. The black dashed line represents the Schottky-Mott equation using an electron affinity value of 4.05 eV.

Journal of Vacuum Science Technology A
ACCEPTED MANUSCRIPT
This is the author's peer reviewed, accepted manuscript. However, the online version of record will be different from this version once it has been copyedited and typeset.
PLEASE CITE THIS ARTICLE AS DOI: 10.1116/6.0000877

where Φ_M is the work function of the metal and χ_S is the electron affinity of the semiconductor; in this case χ_S for β-Ga_2O_3 was assumed to be 4.05 eV [38].

According to the seminal study by Kurtin et al. [49], Ga_2O_3 is expected to closely follow this predicted Schottky-Mott behavior due to its high degree of ionicity; that is, the slope of the plot, $S = \frac{d\phi_B}{d\phi_M}$, termed the index of interface behavior, should be close to 1.00. However, much research since that time has shown other factors can play a dominant role: for example, large variations in S values for different surface planes of the same semiconductor, e.g., SiC and Ga_2O_3, or for different forms of the same semiconductor, e.g., SnS and diamond/NCD [50]. A least-squares fit to each set of data produced the following lines:

$$\phi_B^{JV} = 0.70\phi_M - 2.31\ eV\ , R^2 = 0.89 \quad (10)$$
$$\phi_B^{CV} = 0.97\phi_M - 3.50\ eV, R^2 = 0.89 \quad (11)$$

The corresponding S values are S_{JV} = 0.70 and S_{CV} = 0.97. Further, for the two data points from J-V-T measurements, S_{JVT} = 0.82.

As discussed earlier, differences between Schottky barrier heights (and therefore, S values) calculated from different measurement methods can be attributed to the presence of Schottky barrier inhomogeneities, particularly for the contacts (Pd and Au) with higher ideality factors. Overall, however, the results from this study on (100) β-Ga_2O_3 reveal a strong positive correlation between the calculated Schottky barrier heights and the work function of the metal contacts. In contrast, previous studies of metal contacts to $(\bar{2}01)$ β-Ga_2O_3 did not demonstrate a discernable correlation between Schottky barrier height and metal work function [18, 20], whereas results on (010) β-Ga_2O_3 have been mixed [21, 32]. Hou et al. [20] attribute the strong Fermi level pinning on the $(\bar{2}01)$ Ga_2O_3 surface to its higher oxygen dangling bond density and oxygen vacancies. Our conclusion from the present study in comparison with previous studies discussed above is that due to the surface plane/orientation of β-Ga_2O_3 has a significant effect on the electrical properties (e.g., Schottky barrier height) of metal contacts to this ultra-wide bandgap semiconductor.

IV. SUMMARY

In summary, Ti, Mo, Co, Ni, Pd, and Au Schottky contacts to (100) Czochralski-grown β-Ga_2O_3 were electrically characterized via J-V, C-V, and/or J-V-T measurements. Analysis of the measurements revealed a strong correlation between the calculated Schottky barrier heights and the metal work functions. The electrical behavior of the Au and Pd contacts are associated with the presence of spatially inhomogeneous Schottky barriers, which require further investigation.

ACKNOWLEDGMENTS

This material is based upon work supported by the Air Force Office of Scientific Research (Program Manager, Dr. Ali Sayer) under award number FA9550-18-1-0387. This work was partially performed in the framework of GraFOx a Leibniz-Science Campus partially funded by the Leibniz Association.

Data Availability Statement:

The data that support the findings of this study are available from the corresponding author upon reasonable request.

ACCEPTED MANUSCRIPT
Journal of Vacuum Science Technology A
This is the author's peer reviewed, accepted manuscript. However, the online version of record will be different from this version once it has been copyedited and typeset.
PLEASE CITE THIS ARTICLE AS DOI: 10.1116/6.0000877

References

1. C. Janowitz, V. Scherer, M. Mohamed, A. Krapf, H. Dwelk, R. Manzke, Z. Galazka, R. Uecker, K. Irmscher, R. Fornari, M. Michling, D. Schmeißer, J. R. Weber, J. B. Varley, and C. G. V. d. Walle, New J. Phys. **13,** 085014 (2011).
2. Z. Galazka, S. Ganschow, A. Fiedler, R. Bertram, D. Klimm, K. Irmscher, R. Schewski, M. Pietsch, M. Albrecht, and M. Bickermann, J. Cryst. Growth **486**, 82 (2018).
3. Z. Galazka, K. Irmscher, R. Uecker, R. Bertram, M. Pietsch, A. Kwasniewski, M. Naumann, T. Schulz, R. Schewski, D. Klimm, and M. Bickermann, J. Cryst. Growth **404**, 184 (2014).
4. H. Aida, K. Nishiguchi, H. Takeda, N. Aota, K. Sunakawa, and Y. Yaguchi, Japanese J. Appl. Phys. **47**, 8506 (2008).
5. Z. Galazka, K. Irmscher, R. Schewski, I. M. Hanke, M. Pietsch, S. Ganschow, D. Klimm, A. Dittmar, A. Fiedler, T. Schroeder, and M. Bickermann, J. Cryst. Growth **529**, 125297 (2020).
6. H. Murakami, K. Nomura, K. Goto, K. Sasaki, K. Kawara, Q. T. Thieu, R. Togashi, Y. Kumagai, M. Higashiwaki, A. Kuramata, S. Yamakoshi, B. Monemar, and A. Koukitu, Appl. Phys. Exp. **8**, 015503 (2015).
7. Z. Galazka, Semicon Sci Tech **33** (2018).
8. J. D. Blevins, K. Stevens, A. Lindsey, G. Foundos, and L. Sande, IEEE Trans. Semicon. M. **32**, 466 (2019).
9. K. Konishi, K. Goto, H. Murakami, Y. Kumagai, A. Kuramata, S. Yamakoshi, and M. Higashiwaki, Appl. Phys. Lett. **110** (2017).
10. L. A. M. Lyle, S. Okur, V. S. N. Chava, M. L. Kelley, R. F. Davis, G. S. Tompa, M. V. S. Chandrashekhar, A. B. Greytak, and L. M. Porter, J. Electron. Mat. (2020).
11. L. A. M. Lyle, Carnegie Mellon University (2020).
12. Z. Liu, P.-G. Li, Y.-S. Zhi, X.-L. Wang, X.-L. Chu, and W.-H. Tang, Chinese Phys B **28** (2019).
13. L. A. M. Lyle, L. Jiang, K. K. Das, and L. M. Porter, in *Gallium Oxide – Technology, Devices and Applications*, edited by S. J. Pearton, F. Ren and M. A. Mastro (Elsevier, 2019), pp. 231.
14. C. Fares, F. Ren, and S. J. Pearton, ECS J. Solid State Sc. **8**, Q3007 (2018).
15. D. Splith, S. Müller, F. Schmidt, H. von Wenckstern, J. J. van Rensburg, W. E. Meyer, and M. Grundmann, Phys. Status Solidi A **211**, 40 (2014).
16. K. Irmscher, Z. Galazka, M. Pietsch, R. Uecker, and R. Fornari, J. Appl. Phys. **110** (2011).
17. M. Mohamed, K. Irmscher, C. Janowitz, Z. Galazka, R. Manzke, and R. Fornari, Appl. Phys. Lett. **101**, 132106 (2012).
18. Y. Yao, R. Gangireddy, J. Kim, K. K. Das, R. F. Davis, and L. M. Porter, J. Vac. Sci. Technol B **35** (2017).
19. M. J. Tadjer, V. D. Wheeler, D. I. Shahin, C. R. Eddy, and F. J. Kub, ECS J.Solid State Sc. **6**, P165 (2017).
20. C. Hou, R. M. Gazoni, R. J. Reeves, and M. W. Allen, Appl. Phys. Lett. **114** (2019).
21. C. Hou, R. M. Gazoni, R. J. Reeves, and M. W. Allen, IEEE Electron Dev. Lett. **40**, 337 (2019).

Journal of Vacuum Science Technology A ACCEPTED MANUSCRIPT
This is the author's peer reviewed, accepted manuscript. However, the online version of record will be different from this version once it has been copyedited and typeset.
PLEASE CITE THIS ARTICLE AS DOI: 10.1116/6.0000877

22. Z. Hu, Q. Feng, Z. Feng, Y. Cai, Y. Shen, G. Yan, X. Lu, C. Zhang, H. Zhou, J. Zhang, and Y. Hao, Nanoscale Res. Lett. **14**, 2 (2019).
23. A. Kuramata, K. Koshi, S. Watanabe, Y. Yamaoka, T. Masui, and S. Yamakoshi, Japanese J. Appl. Phys. **55** (2016).
24. K. Shimamura, E. G. Víllora, T. Ujiie, and K. Aoki, Appl. Phys. Lett. **92** (2008).
25. M. Mohamed, C. Janowitz, I. Unger, R. Manzke, Z. Galazka, R. Uecker, R. Fornari, J. R. Weber, J. B. Varley, and C. G. Van de Walle, Appl. Phys. Lett. **97** (2010).
26. N. Suzuki, S. Ohira, M. Tanaka, T. Sugawara, K. Nakajima, and T. Shishido, Phys. Status Solidi C **4**, 2310 (2007).
27. Y. Yao, A. M. L. Luke, A. R. Johanne, O. Serdal, A. T. Gary, S. Tom, S. Nick, F. D. Robert, and M. P. Lisa, ECS Trans. **80**, 191 (2017).
28. Y. Yao, S. Okur, L. A. M. Lyle, G. S. Tompa, T. Salagaj, N. Sbrockey, R. F. Davis, and L. M. Porter, Mat. Res. Lett. **6**, 268 (2018).
29. S. Bin Anooz, R. Grüneberg, C. Wouters, R. Schewski, M. Albrecht, A. Fiedler, K. Irmscher, Z. Galazka, W. Miller, G. Wagner, J. Schwarzkopf, and A. Popp, Appl. Phys. Lett. **116** (2020).
30. S. Bin Anooz, R. Grüneberg, T. S. Chou, A. Fiedler, K. Irmscher, C. Wouters, R. Schewski, M. Albrecht, Z. Galazka, W. Miller, J. Schwarzkopf, and A. Popp, J. Phys. D **54** (2021).
31. K. D. Leedy, K. D. Chabak, V. Vasilyev, D. C. Look, J. J. Boeckl, J. L. Brown, S. E. Tetlak, A. J. Green, N. A. Moser, A. Crespo, D. B. Thomson, R. C. Fitch, J. P. McCandless, and G. H. Jessen, Appl. Phys. Lett. **111** (2017).
32. E. Farzana, Z. Zhang, P. K. Paul, A. R. Arehart, and S. A. Ringel, Appl. Phys. Lett. **110** (2017).
33. K. Jiang, L. A. M. Lyle, E. V. Favela, D. Moody, T. Lin, K. K. Das, A. Popp, Z. Galazka, G. Wagner, and L. M. Porter, ECS Trans. **92**, 71 (2019).
34. L. Du, Q. Xin, M. Xu, Y. Liu, W. Mu, S. Yan, X. Wang, G. Xin, Z. Jia, X.-T. Tao, and A. Song, IEEE Electron Dev. Lett. **40**, 451 (2019).
35. G. Jian, Q. He, W. Mu, B. Fu, H. Dong, Y. Qin, Y. Zhang, H. Xue, S. Long, Z. Jia, H. Lv, Q. Liu, X. Tao, and M. Liu, AIP Adv. **8** (2018).
36. M. Higashiwaki, K. Sasaki, A. Kuramata, T. Masui, and S. Yamakoshi, Appl. Phys. Lett. **100** (2012).
37. M. Higashiwaki, K. Konishi, K. Sasaki, K. Goto, K. Nomura, Q. T. Thieu, R. Togashi, H. Murakami, Y. Kumagai, B. Monemar, A. Koukitu, A. Kuramata, and S. Yamakoshi, Appl. Phys. Lett. **108** (2016).
38. S. J. Pearton, J. Yang, P. H. Cary, F. Ren, J. Kim, M. J. Tadjer, and M. A. Mastro, Appl. Phys. Rev. **5** (2018).
39. E. Farzana, E. Ahmadi, J. S. Speck, A. R. Arehart, and S. A. Ringel, J. Appl. Phys. **123** (2018).
40. S. K. Cheung, and N. W. Cheung, Appl. Phys. Lett. **49**, 85 (1986).
41. H.-Y. Nie, and Y. Nannichi, Japanese J. Appl. Phys. **30**, 906 (1991).
42. Z. Liliental-Weber, J. Washburn, N. Newman, W. E. Spicer, and E. R. Weber, Appl. Phys. Lett. **49**, 1514 (1986).
43. H. Jung, R. Behtash, J. R. Thorpe, K. Riepe, F. Bourgeois, H. Blanck, A. Chuvilin, and U. Kaiser, Phys. Status Solidi C **6**, S976 (2009).
44. T. Jang, S. N. Lee, O. H. Nam, and Y. Park, Appl Phys. Lett. **88** (2006).
45. S. M. Sze, and K. N. Kwok, *Physics of Semiconductor Devices* 763 (2007).

Journal of Vacuum Science Technology A ACCEPTED MANUSCRIPT
This is the author's peer reviewed, accepted manuscript. However, the online version of record will be different from this version once it has been copyedited and typeset.
PLEASE CITE THIS ARTICLE AS DOI: 10.1116/6.0000877

46. R. T. Tung, Phys. Rev. B Condens. Matter **45**, 13509 (1992).
47. R. F. Schmitsdorf, J. Vac. Sci. Technol. B **15** (1997).
48. J. H. Werner, and H. H. Güttler, J. Appl.Phys. **69**, 1522 (1991).
49. S. Kurtin, T. C. McGill, and C. A. Mead, Phys. Rev. Lett. **22**, 1433 (1969).
50. L.M Porter and J.R. Hajzus, *J. Vac. Sci. Technol. A* 38, 031005 (2020).

Journal of Vacuum Science Technology A
ACCEPTED MANUSCRIPT
This is the author's peer reviewed, accepted manuscript. However, the online version of record will be different from this version once it has been copyedited and typeset.
PLEASE CITE THIS ARTICLE AS DOI: 10.1116/6.0000877

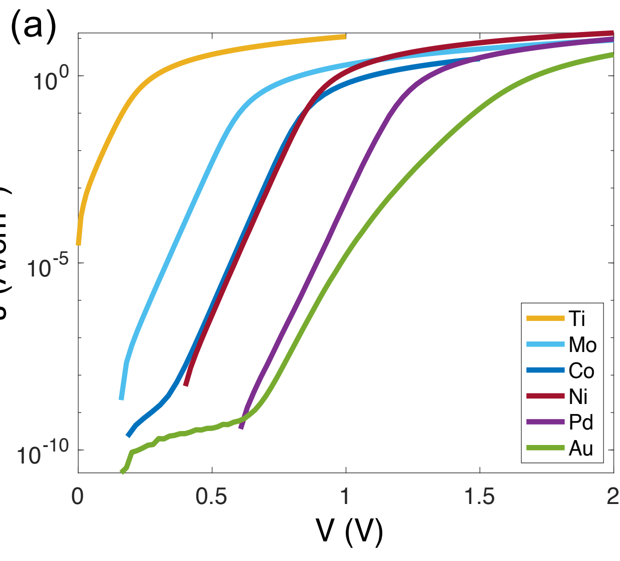

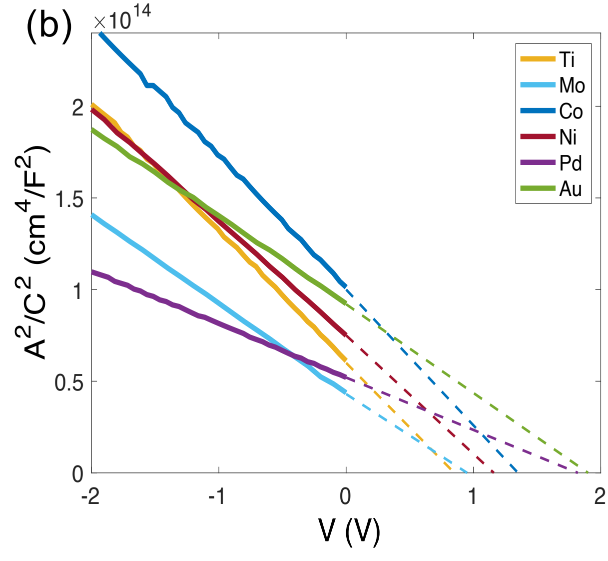

Journal of Vacuum Science Technology A
ACCEPTED MANUSCRIPT
This is the author's peer reviewed, accepted manuscript. However, the online version of record will be different from this version once it has been copyedited and typeset.
PLEASE CITE THIS ARTICLE AS DOI: 10.1116/6.0000877

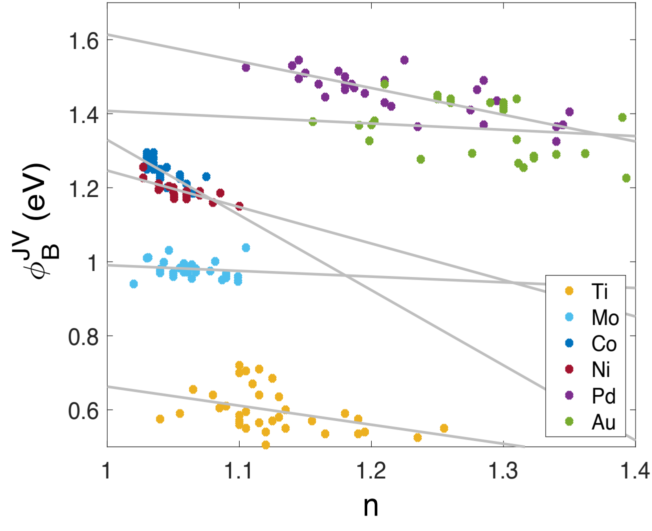

Journal of Vacuum Science Technology A
ACCEPTED MANUSCRIPT
This is the author's peer reviewed, accepted manuscript. However, the online version of record will be different from this version once it has been copyedited and typeset.
PLEASE CITE THIS ARTICLE AS DOI: 10.1116/6.0000877

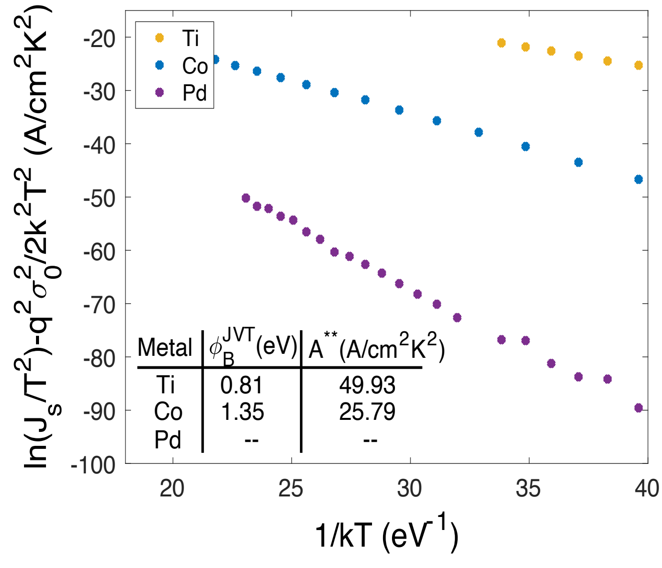

Journal of Vacuum Science Technology A
ACCEPTED MANUSCRIPT
This is the author's peer reviewed, accepted manuscript. However, the online version of record will be different from this version once it has been copyedited and typeset.
PLEASE CITE THIS ARTICLE AS DOI: 10.1116/6.0000877